Three-dimensional integral imaging low light polarimetric image restoration

Kashif Usmani¹, Pranav Wani¹, Timothy O'Connor², and Bahram Javidi¹

¹Electrical and Computer Engineering Department, University of Connecticut, 371 Fairfield Road, Storrs, Connecticut 06269, USA

²Biomedical Engineering Department, University of Connecticut, Storrs, CT, 06269, USA.

*Bahram.Javidi@UConn.edu

Abstract: We overview the enhancement of polarimetric imaging in degraded environments using denoising convolutional neural network model with 3D integral imaging. The experimental results were compared with total variation denoising in terms of SNR and SSIM.

1. System Overview

In this paper, we overview our recently reported work [1] on object visualization of polarimetric imaging for 2D and 3D integral imaging in degraded environments of low light and under partial occlusions using a denoising convolution neural network (DnCNN). Due to its ability to improve the contrast of object scenes from the background, passive polarimetric imaging can be used for object recognition and classification [2-4]. However, polarimetric imaging in low light conditions can become a challenging task due to the saturation of noise during the nonlinear calculation of degree of linear polarization (DoLP). Therefore, improving the signal-to-noise ratio in conventional imaging prior to determining the degree of linear polarization (DoLP) is highly desirable. Three-dimensional integral imaging is a prominent technique that improves the signal-to-noise ratio in low-light environments due to being optimal in the maximum likelihood sense for read noise-dominant images [5-7]. Here, we overview the performance of DnCNN to improve the quality of passive polarimetric imaging in degraded environments of low light under partial occlusions. We compared the reconstructed polarimetric images in low light conditions using DnCNN and total variation (TV) denoising by comparing the signal-to-noise ratio (SNR) and structural similarity index (SSIM) for both 2D and 3D polarimetric imaging scenarios. Our experimental results indicate that the recovered images using DnCNN outperform the recovered images using total variation denoising in terms of SNR and SSIM.

A passive polarimetric integral imaging system as shown in Fig.1 was used to capture the 3D polarimetric information of a scene in degraded environments. A rotating linear polarizer filter is attached with a sensor to record the Stokes parameters. The Stokes parameters in terms of intensity image are defined as $S_0 = I^{0^0} + I^{90^0}$, $S_1 = I^{0^0} - I^{90^0}$, $S_2 = I^{45^0} - I^{135^0}$. These Stokes parameters were used to extract the polarimetric information of a scene in terms of the degree of linear polarization (DoLP). For three-dimensional polarimetric integral imaging, a synthetic aperture integral imaging setup was used. The pickup process of polarimetric integral imaging is shown in Fig. 1(a) and the reconstruction of 3D polarimetric imaging is done via synthetic aperture integral imaging (SAII) by using multiple perspectives of 2D elemental images as shown in Fig. 1(b).

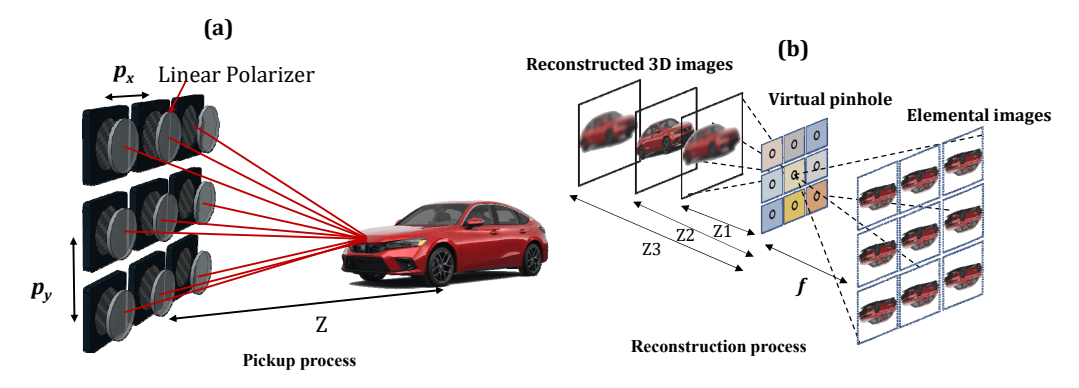


Fig.1. Experimental setup for 3D polarimetric integral imaging. (a) Pick up process, (b) reconstruction process.

The computational 3D polarimetric imaging of the scene at depth z is reconstructed according to the following equation [8]:

$$I_{z}^{\theta}(x,y) = \frac{1}{O(x,y)} \sum_{m=0}^{M-1} \sum_{n=0}^{N-1} \left[I_{m,n}^{\theta} \left(x - \frac{m \times L_{x} \times p_{x}}{c_{x} \times z / f}, y - \frac{n \times L_{y} \times p_{y}}{c_{y} \times z / f} \right) + \varepsilon \right].$$
 (1)

In Eq. (1), M and N are the total numbers of elemental images in horizontal (H) and vertical (V) directions, respectively. (x, y) is the pixel index and O(x, y) is the overlapping pixel number on (x, y). $I^{\theta}_{m,n}$ is the set of polarimetric elemental images with multiple directions θ [0°, 45°, 90°, 135°] while the subscripts m, n represent the location of the elemental image, and p_x and p_y are the camera pitch size in x- and y- directions, respectively. L_x and L_y are the total numbers of pixels in each column and row of images. $c_x \times c_y$ is the pixel size of the camera, z is the pickup distance between the scene and the camera, f is the focal length of a camera lens, and ε is the additive camera noise.

We trained Denoising convolutional neural network (DnCNN) to enhance the visualization of polarimetric imaging. The input for DnCNN consists of a simulated low light noisy polarimetric image, denoted as $y = \alpha x + v$, in which y represents the noisy observation of the ideal polarimetric image x (ground truth), α signifies the degradation parameter, and v represents the additive Gaussian noise originating from the camera sensor. It is designed to predict the noise at each pixel of the residual image (difference between noisy image and latent clean image) rather than directly outputting the denoised image. The residual learning framework is employed to train the residual mapping R(y) between the deformation map (residual image) and the degraded input. Consequently, we obtain x = y - R(y). The loss function $l(\Theta)$ in Equation 2 below is the averaged mean square error between the residual images and the estimated one from degraded input [9]:

$$l(\mathbf{\theta}) = \frac{1}{2k} \sum_{i=1}^{k} \left(\left| \mathbf{R}(\mathbf{y}_i; \mathbf{\theta}) - \left(\mathbf{y}_i - \mathbf{x}_i \right) \right|^2 \right)$$
 (2)

The loss function represented by Equation 2 is utilized to learn the adjustable parameters θ within DnCNN. Here, (y_i, x_i) denotes the pair of noisy and clean image patches extracted from the training images, while k signifies the total number of image pairs. The trained DnCNN network is tested on different polarimetric scenes under different low light conditions with estimated photons per pixel ranging from 2-20 photons/pixel [1].

2. Conclusion

In summary, we overviewed our recently reported work [1] that was based on DnCNN model using 3D polarimetric integral imaging for object visualization different conditions of low light ranging from 2-20 photons/pixel. We compared the recovered polarimetric images in low light conditions using DnCNN and TV denoising by comparing SNR and SSIM. The quantitative metrics SNR, and SSIM indicate that DnCNN model with 3D polarimetric imaging outperforms the 2D polarimetric imaging as well as recovered images using total variation for 2D and 3D polarimetric imaging. B. Javidi acknowledges support by Air Force Office of Scientific Research (FA9550-21-1-0333), Office of Naval Research (N000142212375, N00014-22-1-2349), and National Science Foundation grant number (2141473). We wish to thank Hamamatsu Photonics K. K. for the C11440-42U camera.

References

- K.Usmani, T. O'Connor, and B. Javidi, "Three-dimensional polarimetric image restoration in low light with deep residual learning and integral imaging", Opt. Express 29(8), 29505-29517 (2022).
- 2. K. Usmani, G. Krishnan, T. O'Connor, and B. Javidi, "Deep learning polarimetric three-dimensional integral imaging object recognition in adverse environmental conditions," Opt. Express 29(8), 12215–12228 (2021).
- K. Usmani, T. O'Connor, X. Shen, P. Marasco, A. Carnicer, D. Dey, and B. Javidi, "Three-dimensional polarimetric integral imaging in photon-starved conditions: performance comparison between visible and long wave infrared imaging," Opt. Express 28(13), 19281–19294 (2020).
- 4. X. Shen, A. Carnicer, and B. Javidi, "Three-dimensional polarimetric integral imaging under low illumination conditions," Opt. Lett. 44(13), 3230–3233 (2019).
- 5. G. Lippmann, "Epreuves reversibles donnant la sensation du relief," J. Phys. 7(1), 821–825 (1908).
- B. Tavakoli, B. Javidi, and E. Watson, "Three-dimensional visualization by photon counting computational integral imaging," Opt. Express 16(7), 4426–4436 (2008).
- A. Markman, X. Shen, and B. Javidi, "Three-dimensional object visualization and detection in low light illumination using integral imaging," Opt. Lett. 42(16), 3068–3071 (2017).
- 8. J. S. Jang and B. Javidi, "Three-dimensional synthetic aperture integral imaging," Opt. Lett. 27(13), 1144–1146 (2002).
- 9. K. Zhang, W. Zuo, Y. Chen, D. Meng, and L. Zhang, "Beyond a Gaussian denoiser: Residual learning of deep CNN for image denoising," IEEE Trans. Image Process. 26(7), 3142–3155 (2017).